SPANDIDOS PUBLICATIONS

Abnormal DNA end-joining activity in human head and neck cancer

KI-HYUK SHIN[1,2], MO K. KANG[1,2], REUBEN H. KIM[1], AYAKO KAMETA[1], MARCEL A. BALUDA[1,3] and NO-HEE PARK[1,2,3]

[1]UCLA School of Dentistry; [2]Jonsson Comprehensive Cancer Center; [3]David Geffen School of Medicine at UCLA, Los Angeles, CA 90095, USA

Received November 17, 2005; Accepted December 29, 2005

Abstract. In human cells, DNA double-strand breaks (DSBs) are repaired primarily by the DNA end-joining (EJ) process and thus, abnormal DNA EJ activities lead to an accumulation of mutations and/or aneuploidy, resulting in genetic instability of cells. Since genetic instability is the hallmark of cancer cells, we studied the DNA EJ activities of normal, non-malignant immortalized and malignant human epithelial cells to investigate the association between DNA EJ and carcinogenesis. We found a significant diminution of precise (error-free) DNA EJ activities in non-malignant immortalized human oral keratinocytes (HOK-16B) and human head and neck squamous cell carcinoma (HNSCC) cells compared to that in normal human oral keratinocytes (NHOK). Moreover, abnormal DNA EJ activities were detected exclusively in HOK-16B and HNSCC cells due to microhomology-mediated and non-microhomology-mediated end-joining activities in these cells. These data indicated that aberrant DNA EJ activity may be partly responsible for genetic instability and oncogenic transformation.

Introduction

In mammalian cells, DNA double-strand breaks (DSBs) can be repaired by two distinct and complementary mechanisms, namely homologous recombination (HR) and non-homologous end-joining (NHEJ). In the HR pathway, an undamaged sister-chromatid or homologous chromosome serves as a template for the DSB repair (1). This is the most precise form of repair. In the NHEJ pathway, which is considered the dominant DSB repair mechanism in humans, DSBs are rejoined with the use of little or no homology (1). The NHEJ process is dependent on several cellular factors, including the two subunits of Ku protein, the DNA-dependent protein kinase catalytic subunit (DNA-PKcs), DNA ligase IV (DNL IV) and XRCC4 (2,3). Ku and DNA-PKcs carry out the initial recognition of broken DNA ends, and a complex of DNL IV and XRCC4 catalyzes the formation of phosphodiester bonds.

Accurate NHEJ activity is required for the maintenance of genetic stability (1,4). Gene knockout studies using mice deficient in NHEJ-associated factors, e.g. Ku70, Ku80 or DNA-PKcs, showed that impaired NHEJ activity led to a wide spectrum of chromosomal abnormalities (5-10). Hence, abnormal NHEJ activity and the resulting genetic instability can promote neoplastic cell transformation. We previously reported that the transfection of normal human oral keratinocytes (NHOK) with the cloned genome of 'high risk' human papillomavirus type 16 (HPV-16) resulted in the immortalization of the cells (11,12). The HPV-immortalized oral keratinocytes displayed genetic instability that was demonstrated by increased mutation frequencies and various forms of defective DNA repair (13-15). Genetic instability is generally thought to be a major contributor to chromosomal abnormalities (16,17) and malignant transformation (18-21). In the current study, we compared the ability to repair DSBs in NHOK, HPV-16-immortalized human oral keratinocytes (HOK-16B) and nine cell lines derived from human head and neck squamous cell carcinomas (HNSCC).

We developed two assay systems to quantitatively determine the DNA EJ activity *in vitro* and *in vivo*. Using these assays, we found a significant reduction of precise DNA EJ activity in HPV-immortalized cells and HNSCC cells compared with that in NHOK. Also, abnormal DNA EJ activity in the HPV-immortalized and HNSCC cells caused DNA EJ products with deletions at the repaired site. Such abnormalities were not detected in the DNA EJ products of NHOK.

Materials and methods

Cells and culture conditions. Primary NHOK were prepared from separated epithelial tissue and serially subcultured in Keratinocyte Growth Medium (KGM; Clonetics) containing 0.15 mM Ca^{++} as described previously (12). The immortalized HOK-16B human oral keratinocyte cell line (11) and nine

Correspondence to: Professor N-H Park, UCLA School of Dentistry, CHS 53-038, 10833 Le Conte Avenue, Los Angeles, CA 90095-1668, USA
E-mail: npark@dent.ucla.edu

Key words: DNA end-joining, double-strand break repair, genetic integrity, head and neck squamous cell carcinoma

Table I. Summary of DNA EJ activities in NHOK, HOK-16B, and HNSCC cell lines.

Cells	Tissue origin	Precise EJ (%)[a]	MEJ (%)[b]	NMEJ (%)[c]	p53 status[d]
NHOK[e]	Gingiva	14.6	0	0	Wild-type
HOK-16B[f]	Gingiva	0.9	45	ND[h]	HPV-16
FaDu	Pharynx	4.1	20	ND	Point mutation
Hep-2[g]	Larynx	5.4	9	ND	HPV-18
SCC-4	Tongue	5.3	5	11.4	Point mutation
SCC-9	Tongue	9.0	3	20.8	Deletion
SCC-15	Tongue	2.2	3	ND	Insertion
Tu-139	Larynx	2.2	65	ND	Deletion
Tu-177	Oral	2.1	10	28.6	Point mutation
183	Oral	2.7	15	ND	Point mutation
1483	Oral	4.6	3	15.7	HPV-18

[a]The relative precise DNA EJ activity was calculated by comparing luciferase activity expressed in cells transfected with the *Nar*I-digested plasmid and that of the uncut plasmid. [b]The relative MEJ activity was calculated by comparing the intensity of the 138 bp fragment with that of all amplified PCR products. [c]The frequency of NMEJ error was derived by calculating the number of *Eco*RI-resistant PCR product as a percentage of the total number of tested PCR product. [d]The p53 status in the cells was described in our previous study (35). [e]Three independent cultures of NHOK were obtained from different donors and used in this study. [f]Non-malignant HPV-immortalized human oral keratinocytes (11). [g]HeLa contaminant (ATCC). [h]ND, not determined.

HNSCC cell lines were used in this study (Table I). HOK-16B cells were cultured in KBM supplemented with a growth factor bullet kit. The SCC-4, SCC-9, SCC-15, Hep-2, and FaDu cancer cell lines were purchased from the American Type Culture Collection (ATCC), and the Tu-139, Tu-177, 183, and 1483 cancer cell lines were kindly provided by Dr G. Clayman (University of Texas Medical Center, Houston, TX) and Dr E. Shillitoe (State University of New York College of Medicine, Syracuse, NY). SCC-4, SCC-9 and SCC-15 were cultured in DMEM/Ham's F12 (Gibco/BRL) supplemented with 10% fetal bovine serum (FBS; Gemini Bioproducts) and 0.4 μg/ml hydrocortisone (Sigma), while 1483, Tu-139 and Tu-177 were cultured in DMEM/Ham's F12 supplemented with 10% FBS. The cell lines HEp-2 and FaDu were grown in MEM (Gibco/BRL) supplemented with 10% FBS.

In vitro DNA end-joining assay. Cells were collected and washed three times in ice cold PBS. The cells were lysed by incubation for 30 min at 4˚C in lysis buffer [1% Triton X-100, 150 mM NaCl, 10 mM Tris pH 7.4, 1 mM EDTA, 1 mM EGTA pH 8.0, 0.2 mM sodium orthovanadate, protease inhibitor cocktail (Boehringer Mannheim)]. The cell lysates were centrifuged at 8000 x g for 10 min at 4˚C, and supernatant containing the cellular protein was collected.

The pCR2.1-TOPO plasmid (Invitrogen) was used to evaluate DNA EJ activities. It contains a unique *Eco*RI site and a unique *Eco*RV site with a microhomologous region of 6 bp (5'-CGGCCG-3') on either side of these restriction sites (Fig. 1A). To create a DNA DSB with overhanging ends, the pCR2.1-TOPO plasmid was completely linearized by *Eco*RI (New England Biolabs) as confirmed by agarose gel electrophoresis. The linearized DNA was subjected to agarose gel electrophoresis and gel purification using the QIAquick Gel Extraction kit (Qiagen). The *in vitro* DNA EJ reactions (20 μl) were carried out with 5 μg total cellular extract and 10 ng linearized plasmid in the presence of 4 μl of 50% PEG and 2 μl of 10X T4 ligase buffer (New England Biolabs; 500 mM Tris-HCl pH 7.5, 100 mM $MgC1_2$, 100 mM DTT, 10 mM ATP and 250 ug/ml BSA) at 37˚C for 2 h. After the EJ reaction, PCR reaction was performed with 3 μl DNA EJ reaction using M13 reverse primer (5'-CAGGAAACAGCT ATGAC-3') and M13 forward primer (5'-GTAAAACGA CGGCCAG-3') to amplify rejoined DNA. The PCR conditions consisted of 30 cycles at 95˚C for 30 sec, 60˚C for 30 sec, and 70˚C for 30 sec. PCR products were separated in 2% agarose gel electrophoresis in TBE buffer and visualized by staining with ethidium bromide.

End-joined DNA mediated by microhomology was amplified as a 138 bp fragment (Fig. 1A). End-joined DNA arising from correct ligation or small sequence alteration was amplified as a band of 186 bp or approximately 186 bp, respectively (Fig. 1A). To discriminate between these bands, the PCR products of ≈186 bp were gel-purified, cloned into pcDNA3.1/V5-His TOPO plasmid (Invitrogen), and transfected into *Escherichia coli* strain TOP10 (Invitrogen). After bacterial transformation, single colony PCR was performed using the M13 primer set. The PCR product was digested with *Eco*RI and electrophoresed on 2% agarose gel to compare the restriction profiles. The PCR band of approximately 186 bp, which was resistant to *Eco*RI digestion, was considered to be the product of abnormal non-microhomology-mediated end-joining (NMEJ) activity. The digested PCR products were considered to result from precise DNA EJ activity.

Blunt-ended DNA was prepared by complete digestion of the pCR2.1/GPR1 plasmid with *Eco*RV (New England Biolabs). This plasmid contained an additional 371 bp of partial GPR1 fragment cloned into a cloning site (overhanging 3' deoxythymidine residues) outside the unique *Eco*RV restriction site within the pCR2.1 backbone. Therefore, end-joined DNA mediated by microhomology was amplified as a 138 bp fragment, whereas end-joined DNA arising from

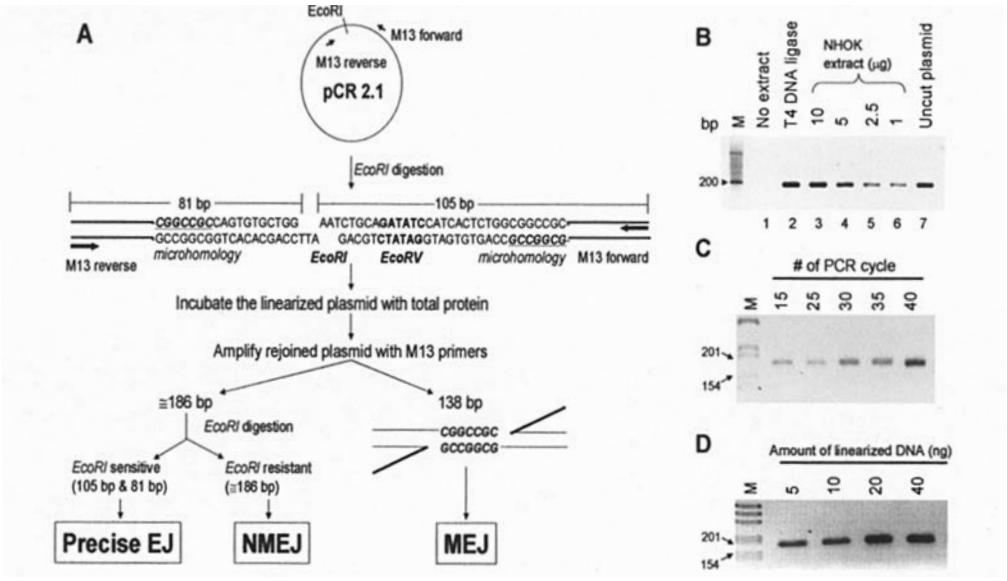

Figure 1. Design and principle of our novel *in vitro* DNA EJ assay. (A) Principle of the assay. This assay permits independent evaluation of precise (error-free) EJ and erroneous EJ (NMEJ and MEJ). (B) DNA EJ catalyzed by NHOK extracts. M, marker; lane 1, no extract (linearized DNA alone); lane 2, T4 DNA ligase; lanes 3-6, different amounts of NHOK extract (10-1 μg); lane 7, uncut plasmid as a PCR control. PCR was performed in 30 cycles. (C) NHOK extract (5 μg) was incubated with 10 ng of linearized DNA, and PCR was carried out with different numbers of cycle. (D) Different amounts of linearized DNA substrate used in the assay. PCR was performed in 30 cycles.

correct ligation or small sequence alteration was amplified as a band of 573 bp or approximately 573 bp, respectively.

DNA sequencing analysis. The 138 bp and *Eco*R1-resistant PCR products were purified with the QIAquick Gel Extraction kit (Qiagen), then sequenced directly with a Taq dideoxy terminator cycle sequencing kit on an ABI 377 automatic DNA sequencer (Perking-Elmer; UCLA Sequencing Core Facility).

Antibody abrogation studies. For immunodepletion, NHOK extract (10 μg) was incubated with various amounts of antisera against ligase IV (Serotec), p53 (Oncogene Sciences) or Ku70 (Serotec) on ice for 30 min. After incubation, the reaction was transferred to 37˚C and incubated for 10 min. The *Eco*RI-linearized DNA substrates (10 ng) were added to the reaction and incubated at 37˚C for 2 h. The *in vitro* DNA EJ assay was then performed, and the products were analyzed by agarose gel electrophoresis as described previously.

In vivo DNA end-joining assay. The pGL3 plasmid (Promega), in which expression of the luciferase gene is controlled by the cytomegalovirus promoter, was used to evaluate correct DNA EJ activity that precisely rejoins broken DNA ends *in vivo*. The pGL3 plasmid was completely linearized by restriction endonuclease *Nar*I (New England Biolabs), which cleaves within the luciferase-coding region as confirmed by agarose gel electrophoresis. The linearized DNA was subjected to phenol/chloroform extraction, ethanol precipitation, and dissolved in sterilized water.

Prior to transfection, a 6-well plate was inoculated with approximately $5x10^4$ cells per well and cultured for 24 h. The cells were then transiently transfected with 1 μg of linearized pGL3 plasmid per well or 1 μg of intact pGL3 plasmid per well using the LipofectAmine reagent (Invitrogen) following the manufacturer's instructions. After 7 h transfection, the transfection medium was replaced with regular culture medium. Cells were collected 48 h after transfection, and cell lysates were prepared according to the Promega instruction manual. Luciferase activity was measured using the Luciferase Reporter Assay System (Promega) and a luminometer (Promega). The reporter plasmid was digested to completion with *Nar*I within the luciferase coding region; only precise DNA end-joining activity should restore luciferase activity. The precise DNA EJ activity was calculated from the luciferase activity of linearized pGL3 plasmids compared with that of uncut plasmids. Each experiment was repeated three times.

Results

HPV-immortalized and HNSCC cells demonstrated abnormal DNA EJ activities in vitro. We developed an *in vitro* PCR-based plasmid end-joining assay that allowed for the quantitative detection of both precise and abnormal DNA EJ activities (Fig. 1A). The pCR2.1 plasmid was linearized at the unique *Eco*RI restriction site to create cohesive DNA ends and incubated with whole cell lysates. Plasmid end-joining was detected by PCR amplification of the plasmid sequence containing the *Eco*RI site, which should yield a 186 bp fragment. To confirm complete digestion of the plasmid DNA and the lack of false amplification resulting from sticky end annealing, the *in vitro* DNA EJ assay was performed without cell lysate. There was no amplification of the substrate DNA without exposure to the cell lysate (Fig. 1B). We also performed the *in vitro* DNA EJ assay with: a) varied amounts of cell lysate; b) varied numbers of PCR amplification cycles; or c) varied amounts of linearized DNA substrate. We found that the level of DNA substrate amplification using the PCR conditions described in this study was quantitatively correlated with these three variables (Fig. 1B-D).

The efficiency and accuracy of *in vitro* DNA EJ activity by whole cell extract from NHOK, immortalized HOK-16B

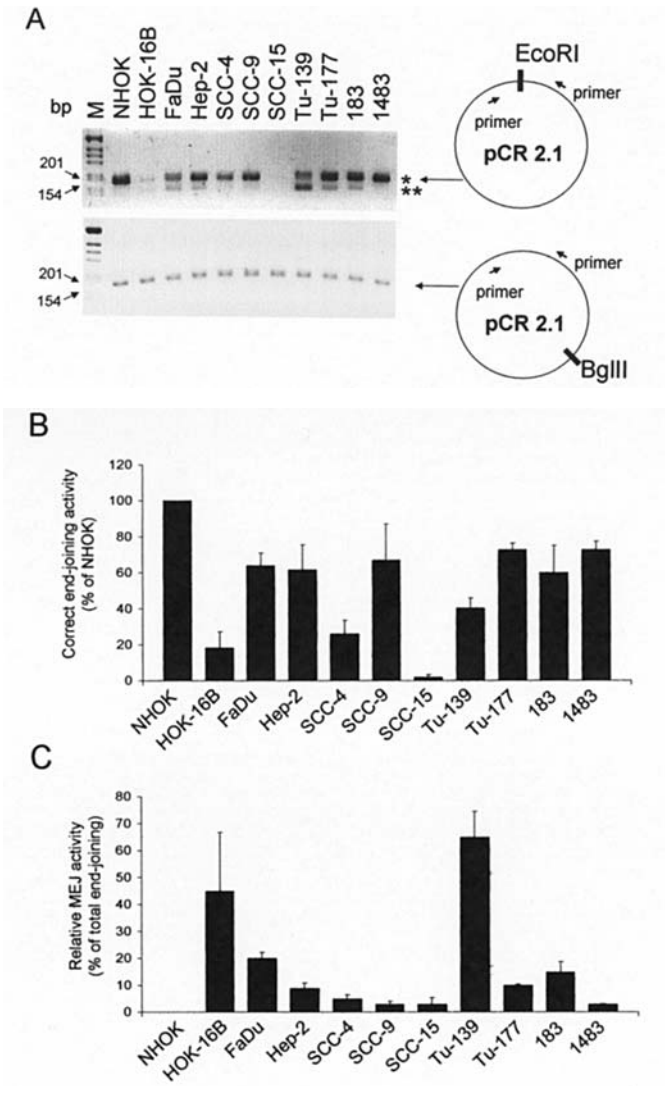

Figure 2. *In vitro* DNA EJ assay. (A) Representative PCR amplification data. Upper panel, the *Eco*RI-linearized plasmid was incubated with cellular extracts and amplified as described in Materials and methods. *Indicates PCR products of 186 bp. **Indicates PCR products of 138 bp resulting from MEJ. Lower panel, the *Bgl*II-linearized plasmid was incubated with cellular extracts and amplified. (B) The relative degree of normal DNA EJ activity was determined from the density of PCR products of approximately 186 bp, which was the expected fragment size from an accurate rejoining process. Graph represents the mean percentage from three independent PCR amplifications. (C) Relative MEJ activity was calculated from the intensity of the 138 bp band compared with that of all amplified PCR products. Graph represents the mean percentage from three independent PCR amplifications.

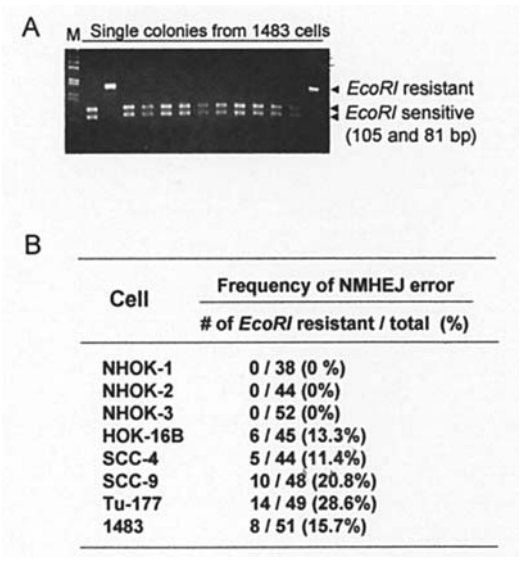

Cell	Frequency of NMHEJ error # of *EcoRI* resistant / total (%)
NHOK-1	0 / 38 (0 %)
NHOK-2	0 / 44 (0%)
NHOK-3	0 / 52 (0%)
HOK-16B	6 / 45 (13.3%)
SCC-4	5 / 44 (11.4%)
SCC-9	10 / 48 (20.8%)
Tu-177	14 / 49 (28.6%)
1483	8 / 51 (15.7%)

Figure 3. Analysis of aberrant NMEJ activity using the *in vitro* DNA end-joining assay. (A) The PCR product from single colony PCR was digested with *Eco*RI and electrophoresed. The PCR product, sensitive to *Eco*RI digestion, indicated precise NMEJ activity. The PCR product, resistant to *Eco*RI-digestion, indicated aberrant NMHEJ activity. (B) NMHEJ frequency in three independent cultures of NHOK, HOK-16B, and four HNSCC cell lines (SCC-4, SCC-9, Tu-177, and 1483). The frequency of the NMHEJ error was calculated by counting the number of *Eco*RI-resistant PCR products as a percentage of the total number of tested PCR products.

cells, or the nine HNSCC cell lines (FaDu, Hep-2, SCC-4, SCC-9, SCC-15, Tu-139, Tu-177, 183, and 1483) were determined as described above. Fidelity of the DNA EJ activity could be partly determined from the size of the PCR products i.e. precise DNA EJ should yield a 186 base pair (bp) fragment, whereas PCR products of different sizes would indicate abnormal DNA EJ activity. However, a minor alteration of the nucleotide sequence at the EJ site, which would destroy the *Eco*RI site, would still yield a fragment of approximately 186 bp (22,23). Strikingly, the cellular extract isolated from NHOK yielded a unique PCR product of 186 bp. In contrast, the HOK-16B line and all of the HNSCC cell lines demonstrated abnormal DNA EJ activity, yielding two PCR products: a fragment of approximately 186 bp and one of 138 bp (Fig. 2A, upper panel). One HNSCC cell line, SCC-15, repeatedly showed barely detectable DNA EJ activity. The degree of precise EJ activity was determined by the intensity of the 186 bp PCR product, which is the expected fragment size of the precise DNA EJ process. The intensity of the 186 bp band in the HOK-16B and HNSCC cells was lower (2.0%-72.8%) compared with that in NHOK (Fig. 2B). In addition, we amplified the *Bgl*II-restricted plasmid to compare the level of consistency among amplification of the regions linearized or not linearized with the unique restriction enzyme (Fig. 2A, lower panel). In this reaction, the amplification of the region not previously linearized (*Bgl*II-restricted plasmid) was consistent among the different cell extracts tested, while that linearized with *Eco*RI showed differential amplification, presumably based on the end-joining efficiency.

To ascertain that the extract from normal cells did not generate the abnormal 138 bp fragment, we performed the assay with cellular extracts from seven independent cultures of NHOK, normal human epidermal keratinocytes, seven different cultures of normal human oral fibroblasts, normal human foreskin fibroblasts (BJ), and normal human lung fibroblasts (IMR-90). The abnormal 138 bp fragment was not detected in any of the assays performed with these normal cells (data not shown).

Abnormal DNA EJ in HPV-immortalized and HNSCC cells resulted from microhomology-mediated and non-microhomology-mediated end-joining activities. To investigate the nature of the abnormal 138 bp fragment generated by the HOK-16B and HNSCC cells, it was isolated and sequenced

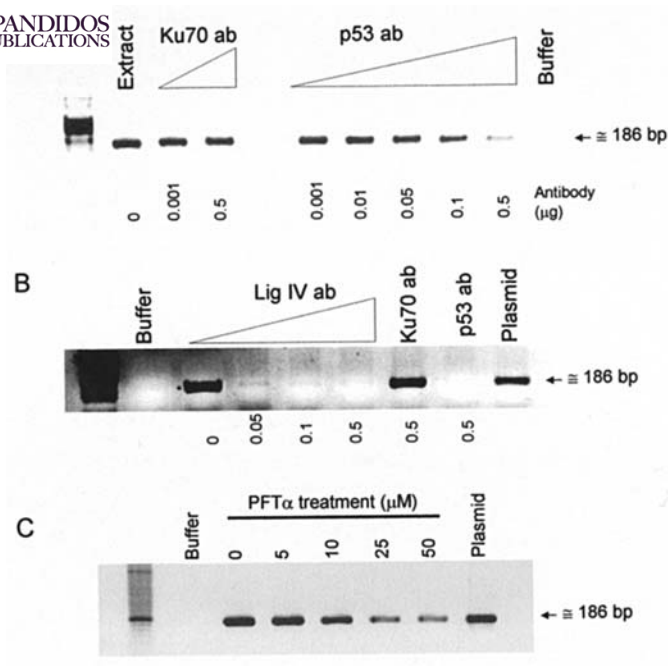

Figure 4. Involvement of ligase IV and p53 in the *in vitro* DNA EJ assay. (A) NHOK extract was treated with various amounts of antibodies against Ku70 (Serotec) or p53 (Oncogene). PCR was performed and PCR products were analyzed by agarose gel electrophoresis. (B) NHOK extract was treated with various amounts of antibodies against ligase IV (Serotec). PCR was performed, and PCR products were analyzed by agarose gel electrophoresis. (C) NHOKs were treated with the indicated concentrations of PFTα for 24 h and harvested. *In vitro* DNA EJ assay was performed using cellular extracts prepared from PFTα-treated NHOK.

after its generation by extracts from HOK-16B, FaDu, Hep-2, Tu-139, Tu-177, and 183 cell lines. All of these 138 bp fragments resulted from the deletion of 48 bp between two microhomologous sequences (5'-CGGCCGC-3') located in the vicinity of the *EcoR*I restriction site (Fig. 1A and sequencing data not shown). Therefore, part of the abnormal DNA EJ activity in the HOK-16B and HNSCC cells occurred through a microhomology-mediated end-joining (MEJ). The relative MEJ activities in NHOK, HOK-16B, and HNSCC cell lines were estimated from the intensity of the 138 bp band compared with that of all amplified PCR products. As shown in Fig. 2C, the MEJ activity accounted for 3-65% of the total EJ activity in the transformed cells. This abnormal MEJ activity in HNSCC cells was also observed with blunt ended DNA substrate after digestion of the pCR2.1 plasmid with *EcoR*V, indicating that the abnormal MEJ activity was not restricted to cohesive overlapping DNA ends (data not shown).

The nature of the approximately 186 bp fragment generated by the tumor cells was investigated to determine whether it contained nucleotide errors at the ligation site by testing its susceptibility to *EcoR*I digestion (22,23). The larger PCR fragment generated by the DNA EJ activity of three independent cultures of NHOK (NHOK-1, -2, and -3), HOK-16B, SCC-4, SCC-9, Tu-177 and 1483 cells was isolated and cloned into the pcDNA3.1/V5-His TOPO plasmid. *E. coli* (TOP10) were transformed with the resulting construct, and a single colony PCR was performed using the M13 primer pair. The PCR products were digested with *EcoR*I and electrophoresed in 2% agarose gel to compare the restriction profiles (Fig. 3A). All PCR products generated by the DNA EJ activity of three independent cultures of NHOK were sensitive to *EcoR*I digestion, indicating precise EJ and correct restoration of the *EcoR*I site (Fig. 3B). In contrast, 6 of 45 (13.3%), 5 of 44 (11.4%), 10 of 48 (20.8%), 14 of 49 (28.6%) and 8 of 51 (15.7%) colonies containing the 186 bp fragment generated by extracts from HOK-16B, SCC-4, SCC-9, Tu-177 and 1483, respectively, were resistant to *EcoR*I digestion (Fig. 3B). The loss of the *EcoR*I restriction site presumably was caused by nucleotide sequence alteration at the EJ site. DNA sequencing analysis of seven randomly selected *EcoR*I-resistant fragments revealed an 8 to 19 bp deletion at the end-joining site (data not shown). However, sequences of microhomology were not found in the vicinity. Thus, the *EcoR*I-resistant fragments represented the occurrence of yet another type of abnormal DNA EJ activity in HOK-16B and the HNSCC cells through a non-microhomology-mediated end-joining (NMEJ) activity (Fig. 1A). This type of abnormal NMEJ activity was absent in the three tested cultures of NHOK.

In vitro DNA EJ assay was ligase IV- and p53-dependent. To determine which major components of the chromosomal DNA EJ process were involved in our *in vitro* PCR-based DNA EJ activity, we tested whether our system was dependent on ligase IV, p53 and Ku70. An NHOK extract was incubated for 30 min on ice with various amounts of polyclonal antibodies against Ku70, ligase IV or p53. After transfer to 37˚C for 10 min, 10 ng of the linearized DNA substrates were added and incubated for 2 h. PCR was then performed and the products were analyzed by agarose gel electrophoresis. As shown in Fig. 4A and B, antisera against ligase IV and p53 inhibited DNA EJ activity. Interestingly, antiserum against Ku70 did not inhibit DNA EJ indicating that under our *in vitro* experimental conditions this supposedly essential component was not required. Thus, Ku70 may be involved in DNA EJ only at the chromosomal level or does not participate in alternative mechanisms of repair. We also tested the inhibitory affect of pifithrin α (PFTα), chemical inhibitor p53, which caused a decrease in amplification of rejoined DNA substrate (Fig. 4C). Thus, our *in vitro* DNA EJ system was dependent on ligase IV and p53, but not on Ku70.

HPV-immortalized cells and HNSCC cells showed reduced precise DNA EJ activity in vivo. Three independent cultures of NHOK (NHOK-1, -2, and -3), HOK-16B, and the nine HNSCC cell lines were transfected with the linearized pGL3-Luc plasmid containing the luciferase reporter gene under control of the CMV promoter. The pGL3-Luc plasmid had been digested to completion with the restriction enzyme *Nar*I at a unique recognition site within the luciferase coding region, creating a DNA DSB with overhanging ends. Thus, luciferase expression in the transfected cells reflected precise (error-free) DNA EJ of the linearized plasmids (23,24). To calculate the precise EJ activity of the tested cells, we also transfected the same cells with uncut circular pGL3-Luc plasmid. To minimize the misinterpretation caused by the cytotoxic effect of DNA and the saturation of luciferase activity, we determined the amount of plasmid expressing

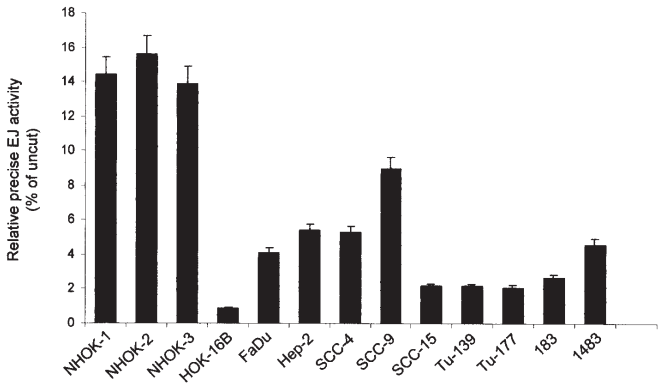

Figure 5. *In vivo* DNA EJ assay. The pGL3-control plasmid contains a unique restriction site, *Nar*I in the luciferase-coding region. The relative precise DNA EJ activity was calculated by comparing luciferase activity expressed in cells transfected with *Nar*I-digested plasmid with that of the uncut plasmid. Three independent cultures of NHOK (NHOK-1, -2, and -3) obtained from different donors, HPV-16 immortalized human oral keratinocytes (HOK-16B), and nine HNSCC cell lines (FaDu, Hep-2, SCC-4, SCC-9, SCC-15, Tu-139, Tu-177, 183, and 1483) were tested. The results were obtained from three independent transfection experiments.

luciferase activity within the linear range by transfecting NHOK with various amounts of the linearized or uncut (circular) pGL3 plasmids. The cells were collected 48 h after transfection and the luciferase activity was measured. The assay revealed that the luciferase activity expressed by 1 μg of the linearized or uncut plasmids were within the linear range of expression (data not shown). Therefore, we used 1 μg of the DNA substrates for the *in vivo* DNA EJ assay.

The relative *in vivo* precise DNA EJ activity was determined from the ratio of luciferase expression in cells transfected with the linearized plasmid and luciferase expression in the same cells transfected with the uncut circular plasmid (Fig. 5). Fifteen percent of the linearized pGL3-Luc plasmids were correctly recircularized in the three NHOK cultures tested, and the efficiency of precise DNA EJ activity was significantly (by the t-test) decreased in all tested HNSCC cells (2-9%) and HOK-16B cells (0.9%). Variation in the efficiency of precise DNA repair in the HNSCC cells is of undetermined origin, but probably resulted form genetic alteration e.g. aneuploidy, gene mutations. We also compared the replication characteristics of the various cell lines with their *in vivo* DNA EJ activities. We did not observe any significant correlation between *in vivo* DNA EJ activity and replication characteristics, such as population doubling time and cell cycle profile (data not shown).

Discussion

Using artificial experimental models of DNA DSB repair, i.e. transient cellular transfection and *in vitro* DNA EJ in cellular extracts, we have separately identified three DNA EJ events that differed between NHOK and transformed or malignant cells with defective p53 activity. In NHOK, we observed that precise DNA EJ accurately rejoined the two DNA DSB ends without any nucleotide alteration, i.e. mutation, addition or deletion, at the EJ site. However, in transformed cells with defective p53 activity, precise DNA EJ was significantly decreased and abnormal DNA EJ occurred: 1) abnormal microhomology-mediated EJ (MEJ) occurred through a seven nucleotide microhomology (25); and 2) abnormal non-microhomology-mediated EJ (NMEJ) is characterized by the deletion of a nucleotide sequence ranging from 8 to 19 base pairs at the rejoined site. The decrease of precise DNA EJ activity and occurrence of abnormal DNA EJ activities were detected in HPV-immortalized, but not malignant HOK-16B cells, and in all nine tested p53-mutated or HPV-infected HNSCC cell lines when compared with NHOK (Table I). While our experimental *in vitro* conditions did not represent actual DNA DSB repair at the chromosomal DNA level, they nevertheless revealed parts of the process involving ligase IV and p53 that are drastically different between normal NHOK and all the malignant HNSCC cells tested. The fact that the *in vitro* DNA EJ reaction was not dependent on Ku70 is consistent with an early role for Ku in DNA damage recognition or repair, i.e. binding DNA ends and attracting the DNA-PK catalytic subunit within the chromosomal DNA-protein complex. This function is either not needed to protect the DNA ends in our *in vitro* system or the Ku-PK activity plays a role in rearranging the chromosomal proteins embedding DNA, which is anchored to the nuclear matrix (26).

The abnormal DNA EJ pathways detected in the HPV-immortalized oral keratinocytes and HNSCC cells, but not in NHOK, indicated that the cellular factors involved in the DNA EJ activity were altered between the normal and transformed oral epithelial cells. Previous studies have shown that several cellular factors participate in the DNA EJ pathway, including p53, Ku70, Ku 80, DNA-PKcs, Rad50, Mre11, Nbs-1, DNA ligase IV and XRCC4 (2,3,26). p53 protein can bind to both double- and single-stranded DNA ends (27-29). Loss of p53-dependent control can dramatically increase genomic instability in animals with Ku80-/-, XRCC4-/- and LigIV-/- genotypes (5,10,30,31). The presence of wild-type p53 enhanced DNA end-joining in irradiated cells when compared with p53 null cells (32,33). Treatment with pifithrin-α, a chemical inhibitor of p53, decreased the accuracy of DNA end-joining activity in mouse fibroblasts, suggesting that p53 facilitates precise repair of DNA DSBs (34). In our recent study, we infected normal human oral fibroblasts (NHOF) with retroviruses expressing wt HPV-16 E6 and examined the cellular DNA EJ activity (23). The cells expressing E6 showed not only diminution of precise DNA EJ, but also an increase in abnormal NMEJ activity when compared with cells without wt E6 (23). Taken together, our data suggest that p53 is an important factor influencing the fidelity of DNA EJ (Table I).

Since the DNA substrates used in this study contained complementary ends created by *Eco*RI digestion, the maintenance of DNA end integrity was critical for the accuracy of DNA EJ. We speculate that the aberrant DNA EJ activity observed in HOK-16B and HNSCC is attributed to inefficient DNA end protection and/or abnormal exonuclease activity either by p53, the MRE complex, or other cellular nucleases. Improper protection of DNA ends at the DSB could have occurred by Ku70/80 malfunction. In our study, p53 was inactivated by either mutation in the DNA binding

SPANDIDOS PUBLICATIONS by HPV infection in all the tested HNSCC cell lines (35). We also detected aberrant DNA EJ activities in HPV-immortalized oral keratinocytes expressing negligible amounts of p53 (11,36). The pleiotropic cellular activities of p53 include DNA end binding and intrinsic 3'→5' exonuclease activities, suggesting a direct association of abnormal or absent p53 activity with aberrant DNA EJ activity (27-29,37-39). This abnormal DNA EJ activity appears to be at the core of defective DNA repair and mutagenesis, which are early steps in the immortalization process of NHOK. Mutagenesis eventually creates the next events or factors, e.g. $p16^{INK4A}$ inactivation, which are necessary for immortalization. This hypothesis explains the delay and infrequent induction of immortalization in NHOK, which survive the M-2 crisis (40). Ectopic expression of a temperature-sensitive p53 mutant in NHOK is mutagenic and extends the *in vitro* cellular replication 4-fold. However, it cannot immortalize the cells, and the temperature-sensitive phenotype of extended life span is reversible before the onset of M-2 crisis (41).

Acknowledgements

Support for this study was provided from grants DE15902 (to K-H.S.) and DE14147 (to N-H.P.) from the National Institute of Dental and Craniofacial Research at the NIH.

References

1. Khanna KK and Jackson SP: DNA double strand breaks: signaling, repair and the cancer connection. Nat Genet 27: 247-254, 2001.
2. Smith GC and Jackson SP: The DNA-dependent protein kinase. Genes Dev 13: 916-934, 1999.
3. Haber JE: Partners and pathways repairing a double-strand break. Trends Genet 16: 259-264, 2000.
4. Schar P: Spontaneous DNA damage, genomic instability, and cancer - when DNA replication escapes control. Cell 104: 329-332, 2001.
5. Ferguson DO, Sekiguchi JM, Chang S, Frank KM, Gao Y, DePinho RA and Alt FW: The nonhomologous end-joining pathway of DNA repair is required for genomic stability and the suppression of translocations. Proc Natl Acad Sci USA 97: 6630-6633, 2000.
6. Zhu C, Bogue MA, Lim DS, Hasty P and Roth DB: Ku80-deficient mice exhibit severe combined immunodeficiency and defective processing of V(D)J recombination intermediates. Cell 86: 379-389, 1996.
7. Gu Y, Jin S, Gao Y, Weaver DT and Alt FW: Ku70-deficient embryonic stem cells have increased ionizing radiosensitivity, defective DNA end-binding activity and inability to support V(D)J recombination. Proc Natl Acad Sci USA 94: 8076-8081, 1997.
8. Karanjawala ZE, Grawunder U, Hsieh CL and Liber MR: The nonhomologous DNA end-joining pathway is important for chromosome stability in primary fibroblasts. Curr Biol 9: 1501-1504, 1999.
9. Lim DS, Vogel H, Willerford DM, Sands AT, Platt KA and Hasty P: Analysis of ku80-mutant mice and cells with deficient levels of p53. Mol Cell Biol 20: 3772-3780, 2000.
10. Difilippantonio MJ, Zhu J, Chen HT, Meffre E, Nussenzweig MC, Max EE, Ried T and Nussenzweig A: DNA repair protein Ku80 suppresses chromosomal aberrations and malignant transformation. Nature 404: 510-514, 2000.
11. Park N-H, Min B-M, Li S-L, Huang MZ, Cherrick HM and Doniger J: Immortalization of normal human oral keratinocytes with type 16 human papillomavirus. Carcinogenesis 12: 1627-1631, 1991.
12. Shin K-H, Min B-M, Cherrick HM and Park N-H: Combined effects of human papillomavirus-18 and N-methyl-N'-nitro-N-nitrosoguanidine on the transformation of normal human oral keratinocytes. Mol Carcinogen 9: 76-86, 1994.
13. Shin K-H, Tannyhill RJ, Liu X and Park N-H: Oncogenic transformation of HPV-immortalized human oral keratinocytes is associated with the genetic instability of cells. Oncogene 12: 1089-1096, 1996.
14. Liu X, Han S, Baluda MA and Park N-H: HPV-16 oncogenes E6 and E7 are mutagenic in normal human oral keratinocytes. Oncogene 14: 2347-2353, 1997.
15. Rey O, Lee S and Park N-H: Impaired nucleotide excision repair in UV-irradiated human oral keratinocytes immortalized with type 16 human papillomavirus genome. Oncogene 18: 6997-7001, 1999.
16. Oda D, Bigler L, Mao EJ and Disteche CM: Chromosomal abnormalities in HPV-16-immortalized oral epithelial cells. Carcinogenesis 17: 2003-2008, 1996.
17. Solinas-Toldo S, Dürst M and Lichter P: Specific chromosomal imbalances in human papillomavirus-transfected cells during progression toward immortality. Proc Natl Acad Sci USA 94: 3854-3859, 1997.
18. Steenbergen RD, Hermsen MA, Walboomers JM, Meijer GA, Baak JP, Meijer CJ and Snijders PJ: Non-random allelic losses at 3p, 11p and 13q during HPV-mediated immortalization and concomitant loss of terminal differentiation of human keratinocytes. Int J Cancer 76: 412-417, 1998.
19. Matthews CP, Shera KA and McDougall JK: Genomic changes and HPV type in cervical carcinoma. Proc Soc Exp Biol Med 223: 316-321, 2000.
20. Sherwood JB, Shivapurkar N, Lin WM, Ashfaq R, Miller DS, Gazdar AF and Muller CY: Chromosome 4 deletions are frequent in invasive cervical cancer and differ between histologic variants. Gynecol Oncol 79: 90-96, 2000.
21. Chuaqui R, Silva M and Emmert-Buck M: Allelic deletion mapping on chromosome 6q and X chromosome inactivation clonality patterns in cervical intraepithelial neoplasia and invasive carcinoma. Gynecol Oncol 80: 364-371, 2001.
22. Kang MK, Shin K-H, Yip FK and Park N-H: Normal human oral keratinocytes demonstrate abnormal DNA end joining activity during replicative senescence. Mech Ageing Dev 126: 475-479, 2005.
23. Shin K-H, Ahn JH, Kang MK, Lim PK, Yip FK, Baluda MA and Park NH: HPV-16 E6 oncoprotein impairs the fidelity of DNA end-joining via p53-dependent and -independent pathways. Int J Oncol 28: 209-215, 2006.
24. Shin K-H, Kang MK, Dicterow E, Kameta A, Baluda MA and Park N-H: Introduction of human telomerase reverse transcriptase to normal human fibroblasts enhances DNA repair capacity. Clin Cancer Res 10: 2551-2560, 2004.
25. Bentley J, Diggle CP, Harnden P, Knowles MA and Kiltie AE: DNA double-strand break repair in human bladder cancer is error prone and involves microhomology-associated end-joining. Nucleic Acids Res 32: 5249-5259, 2004.
26. Kanaar R, Hoeijmakers JH and van Gent DC: Molecular mechanisms of DNA double-strand break repair. Trends Cell Biol 8: 483-489, 1998.
27. Oberosler P, Hloch P, Ramsperger U and Stahl H: p53-catalyzed annealing of complementary single-stranded nucleic acids. EMBO J 12: 2389-2396, 1993.
28. Lee S, Elenbaas B, Levine A and Griffith J: p53 and its 14 kDa C-terminal domain recognize primary DNA-damage in the form of insertion/deletion mismatches. Cell 81: 1013-1020, 1995.
29. Bakalkin G, Selivanova G, Yakovleva T, Kiseleva E, Kashuba E, Magnusson K, Szekely L, Klein G, Terenius L and Wiman K: p53 binds single-stranded DNA ends through the C-terminal domain and internal DNA segments via the middle domain. Nucleic Acid Res 23: 362-369, 1995.
30. Gao Y, Ferguson DO, Xie W, Manis JP, Sekiguchi J, Frank KM, Chaudhuri J, Horner J, DePinho RA and Alt FW: Interplay of p53 and DNA-repair protein XRCC4 in tumorigenesis, genomic stability and development. Nature 404: 897-900, 2000.
31. Frank KM, Sharpless NE, Gao Y, Sekiguchi JM, Ferguson DO, Zhu C, Manis JP, Horner J, DePinho RA and Alt FW: DNA ligase IV deficiency in mice leads to defective neurogenesis and embryonic lethality via the p53 pathway. Mol Cell 5: 993-1002, 2000.
32. Yang T, Namba H, Hara T, Takmura N, Nagayama Y, Fukata S, Ishikawa N, Kuma K, Ito K and Yamashita S: p53 induced by ionizing radiation mediates DNA end-jointing activity, but not apoptosis of thyroid cells. Oncogene 14: 1511-1519, 1997.

33. Tang W, Willers H and Powell SN: p53 directly enhances rejoining of DNA double-strand breaks with cohesive ends in gamma-irradiated mouse fibroblasts. Cancer Res 59: 2562-2565, 1999.
34. Lin Y, Waldman BC and Waldman AS: Suppression of high-fidelity double-strand break repair in mammalian chromosomes by pifithrin-alpha, a chemical inhibitor of p53. DNA Repair 2: 1-11, 2003.
35. Min B-M, Baek JH, Shin K-H, Gujuluva CN, Cherrick HM and Park N-H: Inactivation of the p53 gene by either mutation or HPV infection is extremely frequent in human oral squamous cell carcinoma cell lines. Eur J Cancer 30B: 338-345, 1994.
36. Li S-L, Kim MS, Cherrick HM and Park N-H: Low p53 level in immortal, non-tumorigenic oral keratinocytes harboring HPV-16 DNA. Eur J Cancer 28B: 129-134, 1992.
37. Mummenbrauer T, Janus F, Muller B, Wiesmuller L, Deppert W and Grosse F: p53 protein exhibits 3'-to-5' exonuclease activity. Cell 85: 1089-1099, 1996.
38. Huang P: Excision of mismatched nucleotides from DNA: a potential mechanism for enhancing DNA replication fidelity by the wild-type p53 protein: Oncogene 17: 261-270, 1998.
39. Lilling G, Elena N, Sidi Y and Bakhanashvili M: p53-associated 3'→5' exonuclease activity in nuclear and cytoplasmic compartments of cells. Oncogene 22: 233-245, 2003.
40. Guo W, Kang MK, Kim HJ and Park N-H: Immortalization of human oral keratinocytes is associated with elevation of telomerase activity and shortening of telomere length. Oncol Rep 5: 799-804, 1998.
41. Liu X, Nishitani J, McQuirter JL, Baluda MA and Park N-H: The temperature sensitive mutant p53-143ala extends *in vitro* life span, promotes errors in DNA replication and impairs DNA repair in normal human oral keratinocytes. Cell Mol Biol 47: 1169-1178, 2001.